

Crystal structure refinement and crystal chemistry of pumpellyite

AKIRA YOSHIASA¹ AND TAKEO MATSUMOTO

Department of Earth Sciences, Faculty of Science
Kanazawa University, 1-1 Marunouchi Kanazawa 920, Japan

Abstract

Refinement of the crystal structure of an Al-rich pumpellyite $\{(Ca_{3.86}Na_{0.02}Mn_{0.08})Al_4(Al_{0.93}Fe_{0.46}Mg_{0.67})Si_{60.01}O_{21}(OH)_7; a = 8.812(4) b = 5.895(2) c = 19.116(11)\text{\AA} \beta = 97.41(7)^\circ; \text{space group } A2/m\}$ from Sanbagawa, Gunma Prefecture, Central Japan, was carried out by a least-squares method with X-ray single-crystal counter-collected data. The locations of hydrogen atoms have been determined based on the difference Fourier maps. The final *R* index for 1328 observed reflections is 2.69% for the structure including the hydrogen atoms. All hydrogen positions, located on the mirror planes, are consistent with the results deduced from bond-valence calculations. Hydrogen bonds occur between O(5) and O(10) with a distance of 2.750(4)\AA.

The chemical formula of pumpellyite based on the structure analysis should be written as



and it has the following characters: the double tetrahedral unit $[Si_2O_6(OH)]$ characteristically has a hydroxide group directly attached to the silicate tetrahedron; one of two kinds of octahedral sites is occupied by an aluminum ion in preference to the others; the other octahedral site is occupied by both divalent and trivalent ions such as Fe^{2+} , Mg^{2+} , Fe^{3+} , and Al^{3+} ; and the electric charge of the latter site is compensated by the amount of hydrogen atoms.

Introduction

Pumpellyite occurs commonly in low-grade metamorphic rocks of the pumpellyite-actinolite and prehnite-pumpellyite facies. Gottardi (1965) first proposed the crystal structure model of pumpellyite. Galli and Alberti (1969) tried to refine the structure using film data. In their refinement, however, the temperature factor of the Si(3) atom became negative, and the occupancies of atoms for cation sites were obscured, due to the lack of accurate chemical data. Since then no structure refinement has been done, perhaps due to the poor crystalline nature of the mineral.

Based on the calculations of bond strengths, Allman and Donnay (1971) and Baur (1971) have succeeded in assigning hydrogen atoms to oxygen atoms in the structure model of Galli and Alberti. Their calculations demonstrated that the hydrogen atoms were coupled to O(5), O(7), O(10), and O(11), even though the positions of the hydrogen atoms were not determined. Furthermore, the likelihood of molecular water was excluded.

Various chemical formulae for pumpellyite have been offered by many authors. For instance, Galli and Alberti (1969) showed the following formula on the basis of their crystal structure analysis: $Ca_8Al_8(Mg, Fe^{2+}, Fe^{3+}, Al)_4[(SiO_4)_4/(Si_2O_7)_4/(OH)_8(H_2O, OH)_4]$. From the valence summation procedure, Allman and Donnay (1971)

proposed the following formula for the pumpellyite studied by Galli and Alberti: $Ca_2Al_2(OH)_2(Al, Mg, Fe)(OH, O)Si_4Si_2O_6(OH, O)$. Coombs et al. (1976) used $(Ca, Mn)_4[(Mg, Fe^{2+}, Mn)_{2-x}(Fe^{3+}, Al)_x](Fe^{3+}, Al)_4Si_6O_{20+x}(OH)_{8-x}$ to represent the chemical data from microprobe analysis.

In this study, the structure of pumpellyite has been refined in order to accurately determine the structure parameters and hydrogen positions. Bond-valence calculations are also carried out to ascertain the hydrogen positions. Finally, the crystal chemistry and chemical formula for this mineral are discussed.

Experimental procedure

Material

Through the courtesy of Dr. Kin-ichi Sakurai, we obtained specimens of pumpellyite veins from Oonara, Sanbagawa, Oni-ishi cho, Tano gun, Gunma Prefecture, Central Japan. The species occurs as flat prismatic to bladed crystals up to 0.4 mm in length, elongated along [010] and flattened parallel to (100). The other predominant plane is $(\bar{1}02)$. The fragments show relatively dark-green to pale yellow pleochroism.

Table 1 presents the chemical compositions obtained using a HITACHI XMA-5A electron microprobe analyzer. The chemical compositions vary with the analyzed point from place to place in one grain, and the Fe/(Fe + Mg + Al) atomic ratios for M(2) sites are ca. 0.22. The calculation of the unit cell contents of pumpellyite from microprobe analysis is difficult due to the following reasons: uncertainties of the oxidation state of iron, presence of hy-

¹ Present address: The Institute of Scientific and Industrial Research, Osaka University, Ibaraki, Osaka 567, Japan.

Table 1. Microprobe analyses of pumpellyite

						average
SiO ₂	37.63	37.46	37.48	36.76	36.15	37.10
TiO ₂	0.15	0.12	0.11	0.13	0.01	0.10
Al ₂ O ₃	26.24	25.95	25.92	25.98	25.01	25.82
Fe ₂ O ₃ *	3.68	3.41	3.77	3.90	3.80	3.71
MnO	0.65	0.62	0.51	0.51	0.58	0.58
MgO	2.81	2.84	2.74	2.70	2.85	2.79
CaO	21.97	22.16	22.13	22.15	22.54	22.19
Na ₂ O	0.07	0.06	0.07	0.09	0.09	0.07
K ₂ O	0.02	0.01	0.00	0.01	0.03	0.01
Total**	93.22	92.64	92.73	92.23	91.06	92.37
($\frac{Fe^+}{Mg+Al+Fe^{+1}}$) M(2)-site	0.215	0.207	0.227	0.229	0.236	0.225
Chemical formula***						
Total iron as Fe ₂ O ₃						
(Ca _{3.82} Na _{0.62} Mn _{0.08} Al ₄ (Al _{10.88} Fe _{0.45} Mg _{0.67})Si _{6.95} O ₂₁ (OH) ₇)						
Total iron as FeO						
(Ca _{3.86} Na _{0.02} Mn _{0.08} Al ₄ (Al _{10.93} Fe _{0.46} Mg _{0.67})Si _{6.01} O ₂₁ (OH) ₇)						
* total iron as Fe ₂ O ₃						
**excluding H ₂ O						
*** calculated on the basis of 24.5 oxygens per formula unit						

drogen which is not directly determined, and substitution of O for OH accompanying the introduction of trivalent ions into one of two kinds of octahedral sites (M(2) sites). Because of the above reasons, we employed 24.5 oxygen atoms as the basis for calculation of cell contents of pumpellyite assuming that half of the M(2) sites were occupied by divalent cations. The lower part of Table 1 gives the unit cell content of the mean composition calculated on the basis of total iron as either FeO or Fe₂O₃.

Data collection

The size of the crystal used in the refinement was 0.11 × 0.10 × 0.14 mm³. Weissenberg photographs revealed monoclinic symmetry, and the only observed systematic absence (*hkl*, *k* + *l* = 2*n* + 1) was consistent with space groups *A2/m*, *A2*, and *Am* as previously described (Coombs, 1953, Gottardi, 1965, and Galli and Alberti, 1969). We chose the space group *A2/m* and found the centric model to be satisfactory with regard to agreement between *F*_{obs} and *F*_{calc}. Application of the NZ-test (Howells et al., 1950) also supported the centric model. The data were collected on the Philips PW1100 four-circle diffractometer with graphite-monochromatized MoK α radiation. The unit cell constants determined by the method of least-squares from 20 reflections are given in Table 2, together with other X-ray data.

The intensities of reflections within 2 θ = 8° – 60° were measured in the ω – 2 θ scan mode. A total of 1549 reflections was collected over one asymmetric unit. The data were corrected for Lorentz and polarization factors, and for the absorption effect, the crystal was assumed to be a sphere (μR = 0.15 for MoK α radiation). Reflections were included in the calculations if their structure factors exceeded three standard deviations based on counting statistics. This resulted in 1318 unique reflections.

Table 2. Pumpellyite, X-ray data

a (Å)	8.812(4)
b	5.895(2)
c	19.116(11)
β (°)	97.41(7)
V (Å ³)	984.75
space group	A 2/m
D _{calc} (g·cm ⁻³)	3.23
radiation used	MoK α (0.71069Å)
monochromator	graphite
crystal size (mm)	0.11 × 0.10 × 0.14
μ (cm ⁻¹)	21.61
diffractometer	Philips PW1100
scan type	ω -2 θ
2 θ range (°)	8 – 60
No. of indep. reflections measured	1525
No. of indep. reflections used for refinement with <i>F</i> _o > 3 σ (<i>F</i> _o)	1328
final R	2.69 %
final R _w	2.74 %

Refinement

The refinement was initiated with the positional parameters reported by Galli and Alberti (1969) for the 1318 observed unique structure factors using the program LINUS (Coppens and Hamilton, 1970). Neutral atomic scattering factors (*International Table for X-ray Crystallography*, Vol. 3) were used for each atom. Na and Mn atoms were disregarded in the refinement, since their

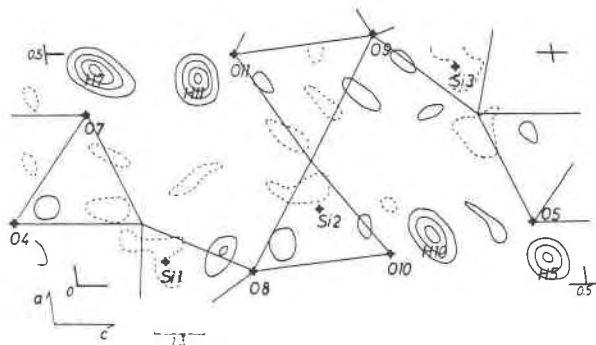


Fig. 1. Portion of the difference Fourier section, *y* = 0.0, of pumpellyite, passing through the hydrogen positions, H5, H7, H10, and H11; neighboring tetrahedra and octahedra formed by oxygen atoms are indicated. Contours are drawn at an interval of 0.2 e/Å³, zero contours being omitted, and negative contours broken. Atoms lying on the plane are indicated by +.

Table 3. Pumpellyite, positional parameters and isotropic temperature factors for hydrogen atoms

atom	site occupancy	x	y	z	B _{iso}
Ca (1)		0.25033 (8)	0.5	0.33962 (4)	
Ca (2)		0.19044 (9)	0.5	0.15453 (4)	
M (2)	0.80 Al 0.20 Fe	0.5	0.25	0.25	
M (1)	1.00 Al	0.25469 (8)	0.24585 (13)	0.49589 (4)	
Si (1)		0.05055 (10)	0.0	0.08966 (5)	
Si (2)		0.16539 (11)	0.0	0.24764 (5)	
Si (3)		0.46524 (10)	0.0	0.40323 (5)	
O (1)		0.13767 (18)	0.22615 (30)	0.07086 (8)	
O (2)		0.26532 (20)	0.23090 (31)	0.24597 (9)	
O (3)		0.36694 (19)	0.22415 (33)	0.41795 (9)	
O (4)		0.13068 (27)	0.5	0.44515 (13)	
O (5)		0.13328 (30)	0.0	0.45015 (15)	
O (6)		0.36919 (27)	0.5	0.04487 (13)	
O (7)		0.36712 (29)	0.0	0.03267 (13)	
O (8)		0.03611 (28)	0.0	0.17546 (12)	
O (9)		0.47856 (29)	0.5	0.17585 (13)	
O (10)		0.06645 (33)	0.0	0.31367 (14)	
O (11)		0.50216 (30)	0.5	0.31488 (14)	
H (5)		0.069 (17)	0.0	0.466 (8)	1.1 (3.0)
H (7)		0.444 (7)	0.0	0.045 (3)	0.3 (1.4)
H (10)		0.092 (13)	0.0	0.343 (6)	5.4 (4.4)
H (11)		0.443 (9)	0.0	0.155 (4)	3.0 (2.2)

Table 4. Pumpellyite, anisotropic temperature factor coefficients for non-hydrogen atoms

atom	β_{11}	β_{22}	β_{33}	β_{12}	β_{13}	β_{23}
Ca (1)	221 (9)	591 (21)	31 (2)	0.0	28 (3)	0.0
Ca (2)	558 (11)	380 (20)	34 (2)	0.0	-9 (3)	0.0
M (1)	165 (9)	315 (21)	33 (2)	8 (10)	22 (3)	-4 (4)
M (2)	289 (11)	479 (25)	55 (2)	12 (12)	32 (3)	4 (6)
Si (1)	150 (10)	418 (23)	34 (2)	0.0	11 (4)	0.0
Si (2)	209 (10)	401 (24)	38 (2)	0.0	-3 (4)	0.0
Si (3)	156 (10)	432 (23)	29 (2)	0.0	16 (4)	0.0
O (1)	253 (18)	450 (43)	55 (4)	-44 (24)	38 (7)	2 (11)
O (2)	381 (20)	498 (44)	59 (4)	-15 (25)	-4 (7)	8 (12)
O (3)	283 (19)	522 (44)	56 (4)	112 (25)	51 (7)	13 (11)
O (4)	201 (26)	500 (61)	53 (6)	0.0	5 (10)	0.0
O (5)	193 (28)	596 (65)	65 (6)	0.0	9 (11)	0.0
O (6)	205 (27)	453 (60)	53 (6)	0.0	-10 (10)	0.0
O (7)	179 (28)	610 (66)	71 (6)	0.0	-4 (11)	0.0
O (8)	203 (27)	1072 (72)	29 (6)	0.0	6 (10)	0.0
O (9)	242 (28)	1330 (79)	48 (6)	0.0	33 (10)	0.0
O (10)	354 (32)	1772 (92)	53 (6)	0.0	22 (11)	0.0
O (11)	281 (30)	1128 (75)	57 (6)	0.0	40 (11)	0.0

$$* \beta_{ij} = \beta_{ji} \times 10^5$$

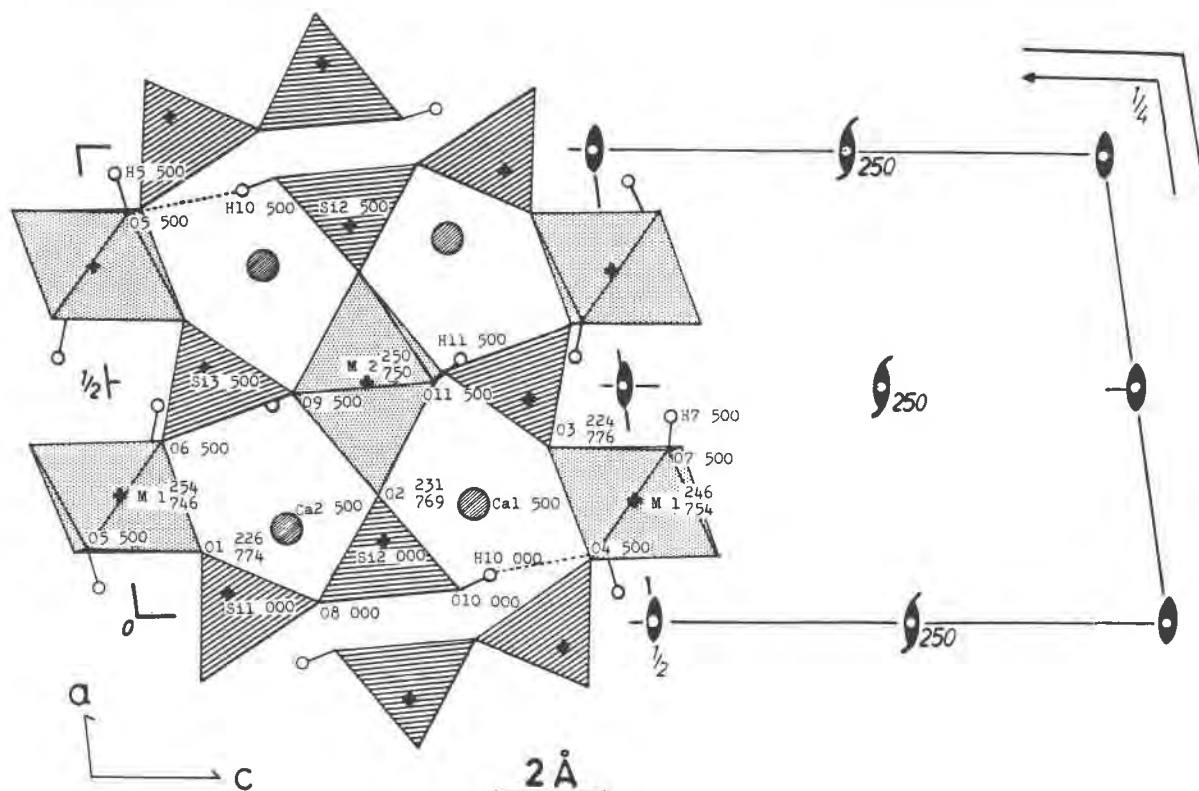


Fig. 2. Pumpellyite, view parallel to [010]. The heights of the atoms are indicated in 1000y. The elements of symmetry are indicated in half of the unit cell.

Table 6. Pumpellyite, interatomic distances (Å) and angles (°)

Ca(1)-polyhedron		M(2)-octahedron		M(2)-octahedron		Si(1)-tetrahedron	
Ca(1)-O(2)	2.408(2)	O(2)-Ca(1)-O(3)	87.51(6)	M(2)-O(2)	2.063(3)	O(2)-M(2)-O(9)	90.63(9)
-O(3)	2.355(2)	O(2)-Ca(1)-O(4)	137.33(5)	-O(9)	2.036(2)	O(2)-M(2)-O(11)	89.54(7)
-O(4)	2.394(3)	O(2)-Ca(1)-O(8)	93.77(6)	-O(11)	1.925(2)	O(9)-M(2)-O(11)	83.49(8)
-O(8)	2.503(3)	O(2)-Ca(1)-O(11)	72.77(7)	Average	2.008		
-O(11)	2.327(3)	O(3)-Ca(1)-O(4)	70.59(6)	O(2)-O(9)	2.914(3)		
Average	2.393	O(3)-Ca(1)-O(8)	115.08(6)	-O(9)	2.883(3)		
		O(3)-Ca(1)-O(11)	77.30(6)	-O(11)	2.810(3)		
		O(4)-Ca(1)-O(8)	63.24(8)	-O(11)	2.832(3)		
		O(4)-Ca(1)-O(11)	134.95(9)	O(2)-O(11)	2.639(4)		
		O(8)-Ca(1)-O(11)	161.82(9)	-O(11)	2.756(4)		
Ca(2)-polyhedron		Si(1)-tetrahedron		Si(1)-tetrahedron		Si(1)-tetrahedron	
Ca(2)-O(1)	2.278(2)	O(1)-Si(1)-O(1)	112.02(10)	Si(1)-O(1)	1.902(2)	O(1)-Si(1)-O(4)	112.13(8)
-O(2)	2.389(2)	O(1)-Si(1)-O(4)	112.13(8)	-O(4)	1.649(2)	O(1)-Si(1)-O(8)	108.75(8)
-O(6)	2.780(3)	O(1)-Si(1)-O(8)	108.75(8)	-O(8)	1.661(3)	O(4)-Si(1)-O(8)	101.81(13)
-O(9)	2.519(3)	O(4)-Si(1)-O(8)	101.81(13)	Average	1.629		
-O(10)	2.419(3)			O(1)-O(1)	2.666(3)		
Average	2.436			-O(4)	2.698(3)		
				-O(8)	2.653(3)	Si(1)-O(8)-Si(2)	133.15(17)
				O(4)-O(8)	2.569(3)		
M(1)-octahedron		Si(2)-tetrahedron		Si(2)-tetrahedron		Si(2)-tetrahedron	
M(1)-O(1)	1.878(2)	O(2)-Si(2)-O(2)	111.42(11)	Si(2)-O(2)	1.624(2)	O(2)-Si(2)-O(8)	107.79(8)
-O(3)	1.896(2)	O(2)-Si(2)-O(8)	107.79(8)	-O(8)	1.672(2)	O(2)-Si(2)-O(10)	111.23(9)
-O(4)	2.026(2)	O(8)-Si(2)-O(10)	105.34(14)	-O(10)	1.624(3)		
-O(5)	1.888(2)			Average	1.636		
-O(6)	1.937(2)			O(2)-O(2)	2.722(3)		
-O(7)	1.882(2)			-O(8)	2.655(3)		
Average	1.918			-O(10)	2.680(3)		
O(1)-O(4)	2.698(3)			O(8)-O(10)	2.621(4)		
-O(5)	2.687(3)						
-O(6)	2.597(3)						
-O(7)	2.604(3)						
O(3)-O(4)	2.744(3)						
-O(5)	2.643(3)						
-O(6)	2.689(3)						
-O(7)	2.730(3)						
O(4)-O(5)	2.958(3)						
-O(7)	2.490(3)						
O(5)-O(6)	2.485(3)						
O(6)-O(7)	2.957(4)						

contents were too small. As the scattering factors of Mg and Al atoms are nearly identical, the octahedral sites were modified so as to be occupied by Al and Fe only. A scattering factor, $(1-g)f(\text{Al}) + gf(\text{Fe})$, was used for the composite atom at the octahedral sites, where $f(\text{Al})$ and $f(\text{Fe})$ are the scattering factors of Al and Fe, respectively, and g is the occupancy factor. The occupancy factors were varied with positional parameters, isotropic extinction parameter, temperature factors, and scale factor. Several cycles of least-squares refinements, gradually increasing the number of variables, resulted in convergence at an R index ($= \sum \|F_o| - |F_c| \| / \sum |F_o|$) of 0.0516 for isotropic temperature factors. Then temperature factors were converted to anisotropic, and several cycles of refinement resulted in convergence at an R index of 0.0291.

After the convergence a difference Fourier synthesis was computed to find the hydrogen atoms of the hydroxyl groups. A portion of the difference Fourier section, $y = 0.0$, is shown in Figure 1 together with the tetrahedra and octahedra formed by neighboring oxygen atoms. The map revealed the hydrogen atoms at distances of about 1 Å from O(5), O(7), O(10), and O(11) for OH, the peak height being 0.6, 0.8, 0.6, 0.8 $\text{e} \text{Å}^{-3}$ respectively.

Upon further refinement including the hydrogen atoms, for which positional parameters and isotropic temperature factors were varied, the R index converged to 0.0269.

Site occupancy showed (0.80 Al + 0.20 Fe) in the centrosymmetric M(2) site, and (1.01 Al + -0.01 Fe) in the M(1) site. The negative occupancy of Fe in the M(1) site suggests that the M(1) site would primarily be occupied by Al.

The positional parameters (Table 3) and the temperature factor coefficients (Table 4) were used to calculate a final set of structure factors (Table 5).² Interatomic distances, angles, and estimated standard errors calculated using RSDA-4 program (Sakurai, 1967) are given in Table 6.

Discussion

Description of the structure

Our structural refinement confirmed the general polyhedral linkage proposed by the earlier studies. The structure contains octahedra which share edges to form infinite

² To receive a copy of Table 5, order Document AM-85-276 from the Business Office, Mineralogical Society of America, 2000 Florida Avenue, N.W., Washington, D.C. 20009. Please remit \$5.00 in advance for the microfiche.

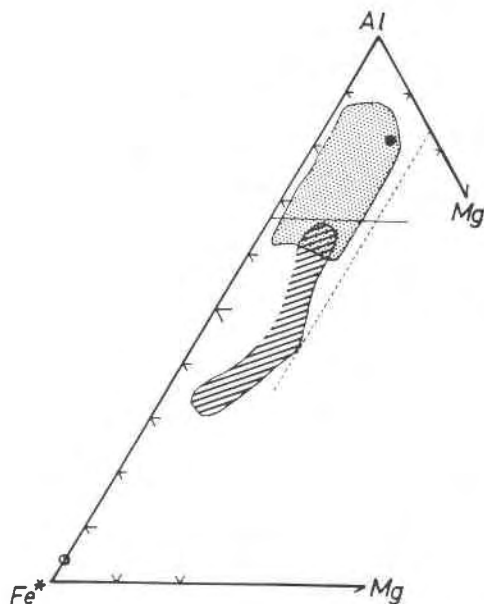


Fig. 3. Pumpellyite compositions from various rock types in the diagram of atomic proportions Al-Mg-Fe*(Fe²⁺ + Fe³⁺). Dashed line indicates Mg/(Al + Mg + Fe*) = 0.167, full line indicates Al/(Al + Mg + Fe*) = 0.667. Solid circle—this study; open circle—(julgoldite) Moore (1971); striped field—(ophiolite members) data from Liou et al. (1977), Liou (1979) and Ishizuka (1981); stippled field—data from Deer et al. (1962), Passaglia and Gottardi (1973), Zen (1974), Kawachi (1975), Coombs et al. (1976), Kuniyoshi and Liou (1976), Aiba (1982), Nakajima (1982), and Arai (pers. comm.)

linear chains parallel to the [010] direction. There are the two symmetrically independent chains, one of which is composed of the M(2) octahedra on a special position, while the other is the M(1) octahedra on the general position. In the unit cell, there are four symmetrically equivalent M(2) sites, and eight M(1) sites, therefore four M(1) chains and two M(2) chains run parallel to [010]. The shared edges in these chains are O(9)–O(11) for the M(2) site, and O(5)–O(6) and O(4)–O(7) for the M(1) site.

The existence of both double tetrahedra Si₂O₆(OH) and isolated tetrahedra SiO₄ is characteristic for this crystal structure. There is no edge shared between the tetrahedra and the octahedra. Tetrahedra which alternate at heights $y = 0.0$ and 0.5 , laterally bridge between O(1)–O(1), O(2)–O(2), and O(3)–O(3) vertices (unshared edges) of the different octahedra. The cross-linking by the octahedra and the tetrahedra exists as shown in Figure 2. This octahedra-tetrahedra linkage therefore results in a three dimensional framework. This framework is sufficiently open to accommodate a calcium atom.

The observed mean Ca–O distances for seven-fold Ca(1) and Ca(2) sites are 2.393 and 2.436 Å respectively. The additional eighth oxygen atoms are located at distances of 3.369 (Ca(1)–O(10) and 3.292 Å (Ca(2)–O(8)). The coordi-

nation polyhedron of seven oxygen atoms around each calcium atom is described as a square with two oxygen atoms on one side and one on the other. Ca(1)-polyhedra share the edges O(3)–O(4) with M(1)-octahedra and the edges O(2)–O(11) with M(2)-octahedra, and the Ca(2)-polyhedra also share the edges O(1)–O(6) with M(1)-octahedra and the edges O(2)–O(9) with M(2)-octahedra (note that the number of sharing edges for the M(2) sites is twice that for the M(1) sites). Ca(1)- and Ca(2)-polyhedra share the edges O(4)–O(8) with Si(1)-tetrahedra and the edges O(6)–O(9) with Si(3)-tetrahedra, respectively.

The polyhedra show the usual effect of sharing edges. The lengths of edges shared between the octahedra, 2.485 and 2.498 Å for M(1)-octahedra and 2.639 Å for M(2)-octahedra, are significantly shorter than the edge lengths parallel to the *b* axis, 2.958 and 2.957 Å and 2.956 Å. In the tetrahedra, the lengths of edges shared by Ca-polyhedra

Table 7. Pumpellyite, magnitude and orientation of principal axes

	Equivalent isotropic temperature factor	Axes	RMS deviation	θ(a)	θ(b)	θ(c*)
Ca(1)	0.69	1	0.095	27	90	63
		2	0.102	90	0	90
		3	0.070	117	90	27
Ca(2)	0.93	1	0.150	6	90	96
		2	0.082	90	0	90
		3	0.078	84	90	6
M(2)	0.77	1	0.109	37	84	53
		2	0.091	94	6	94
		3	0.095	127	89	37
M(1)	0.46	1	0.084	44	89	46
		2	0.075	74	25	108
		3	0.069	129	65	49
Si(1)	0.51	1	0.076	15	90	105
		2	0.086	90	0	90
		3	0.079	75	90	15
Si(2)	0.58	1	0.095	25	90	115
		2	0.084	90	0	90
		3	0.078	65	90	25
Si(3)	0.49	1	0.079	33	90	57
		2	0.087	90	0	90
		3	0.070	123	90	33
O(1)	0.72	1	0.094	65	135	125
		2	0.082	52	47	113
		3	0.108	49	101	44
O(2)	0.91	1	0.126	20	95	109
		2	0.093	90	13	103
		3	0.101	70	77	24
O(3)	0.78	1	0.120	46	63	56
		2	0.078	135	56	65
		3	0.095	97	134	44
O(4)	0.69	1	0.087	22	90	68
		2	0.094	90	0	90
		3	0.106	112	90	22
O(5)	0.79	1	0.087	10	90	80
		2	0.103	90	0	90
		3	0.109	100	90	10
O(6)	0.69	1	0.083	36	90	55
		2	0.089	90	0	90
		3	0.107	126	90	36
O(7)	0.82	1	0.082	18	90	72
		2	0.104	90	0	90
		3	0.117	108	90	18
O(8)	0.85	1	0.089	4	90	94
		2	0.137	90	0	90
		3	0.073	86	90	4
O(9)	1.08	1	0.085	44	90	134
		2	0.153	90	0	90
		3	0.103	46	90	44
O(10)	1.43	1	0.117	9	90	81
		2	0.177	90	0	90
		3	0.098	59	90	9
O(11)	1.07	1	0.093	43	90	133
		2	0.141	90	0	90
		3	0.111	47	90	43

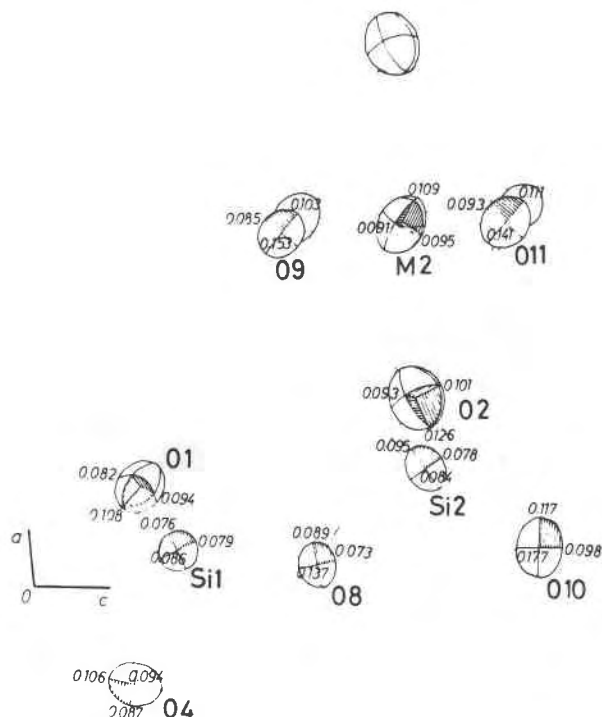


Fig. 4. Projection of magnitude and orientation of principal axes of M(2), Si(1), and Si(2) sites on the (010) plane. Root-mean-square thermal displacements (Å) are shown.

(O(4)–O(8) and O(6)–O(9)) are also shorter than those of the others. Si(1)–O(8) and Si(2)–O(8) bridging bonds are longer than the mean interatomic distance of 1.635 Å for all tetrahedral sites. A combined slight undulation of edge-sharing octahedral chains bridged by tetrahedra (as shown in zoisite and clinozoisite, Dollase (1968)) could be caused by the difference between the tetrahedral edge length and the expected distance to be bridged for the octahedral chains.

Distribution of cations

In pumpellyite, there are two distinct octahedral sites (M(1) and M(2)), two distinct seven-fold polyhedral sites (Ca(1) and Ca(2)), and three distinct tetrahedral sites (Si(1), Si(2), and Si(3)). The M(1) sites are almost completely occupied by Al^{3+} , and M(2) sites are occupied by Mg^{2+} , Fe^{2+} , Fe^{3+} , and Al^{3+} ; that is to say Fe and Mg atoms in this structure are concentrated in the site of higher symmetry of the two octahedral sites. This result is consistent with the distribution which was previously assumed by Galli and Alberti (1969). From site-population refinement, the M(2) site was composed of Al(80%) Fe(20%), and then the $\text{Fe}/(\text{Fe} + \text{Al})$ value of 0.20 was in agreement with the $\text{Fe}/(\text{Fe} + \text{Al} + \text{Mg})$ values of 0.207 ~ 0.236 from microprobe analyses.

The scattering factors of Mg–Al and of Al–Si are very

similar, but the effective ionic radii (Shannon, 1976) of ${}^{\text{vi}}\text{Mg}^{2+}$ (0.720 Å) – ${}^{\text{vi}}\text{Al}^{3+}$ (0.535 Å) and of ${}^{\text{iv}}\text{Al}^{3+}$ (0.39 Å) – ${}^{\text{iv}}\text{Si}^{4+}$ (0.26 Å) are considerably different; the observed mean interatomic distances thus should give some indication of the site occupancies. The mean distances in the octahedral sites (M(1)–O = 1.918 and M(2)–O = 2.008 Å) indicate that Al^{3+} occupies the M(1) sites in preference to any other ions, and that Mg^{2+} , Fe^{2+} , and Fe^{3+} occupy the M(2) sites, in agreement with the site-population refinement. The tetrahedral sites are composed of Si only.

Chemical compositions of pumpellyite reported in the literatures are plotted on a three-component diagram (Fig. 3) of atomic proportion; $\text{Al}:\text{Mg}:\text{Fe}^*$ ($=\text{Fe}^{2+} + \text{Fe}^{3+}$). We can use this diagram to find the ratio of the cations for octahedral sites on the assumption that M(1) sites ($=8/12$)³ are occupied by aluminum (trivalent) ions in preference to any other. It is evident that no specimen exceeds the dashed line of $\text{Mg}/(\text{Al} + \text{Mg} + \text{Fe}^*) = 2/12$; Mg atoms do not occupy over half of M(2) sites ($=4/12$) which are occupied by both divalent and trivalent ions such as Mg^{2+} , Fe^{2+} , Fe^{3+} , and Al^{3+} . If the M(2) sites were separated into two sites by site-preference of Mg ions, or rather by the difference of ionic radius and valence, the space group of pumpellyite would be *A2* or *Am*.

Anisotropic thermal motion

Magnitude and orientation of the principal axes of the thermal ellipsoids are presented in Table 7. The equivalent isotropic temperature factors of the O(2), O(9), O(10), and O(11) oxygen atoms are significantly greater than the others. Among them O(2), O(9), and O(11) form the centrosymmetric octahedron of the M(2) site. The concentration of Fe or Mg atoms occurs in the M(2) site expanding this octahedron. Therefore, it may be emphasized that the displacement of the coordinates of the M(2) octahedra-forming oxygen atoms occurs statistically due to the difference of sizes among the M(2) sites and that this displacement has an effect on apparent temperature factors of these oxygen atoms. The root-mean-square displacements for axis-1 of O(2) and axes-2 of O(9) and O(11) are 0.126, 0.153, and 0.141 Å, respectively (see Fig. 4). The bridging Si(2) tetrahedra pivot on O(8) atoms in proportion to the expansion of M(2) sites; so that the orientation of the ellipsoid of Si(2) approximately correlates with that of O(2).

The ellipsoid of O(10) has its two shorter axes lying in the mirror plane with O(10)–Si(2) and O(11)–Ca(2) bonds and the direction of the greatest vibration is normal to these bonds. The greatest temperature factor of O(10) among all anions in the crystal could be understood from the expansion of M(2) sites and from the fact that O(10) is the single oxygen atom which does not involve the framework of octahedra and tetrahedra.

³ In one unit cell of the mineral there are twelve octahedral sites in all.

Table 8. Interatomic distances (Å) and angles (°) for hydrogen atoms

H(7)-O(7)	0.7(1)	H(5)-O(5)	0.6(2)
H(7)-O(11)	2.7(1)	H(5)-O(5)	2.4(2)
H(7)-O(7)	2.4(1)		
H(11)-O(11)	0.7(1)	H(10)-O(10)	0.6(2)
H(11)-O(7)	2.4(1)	H(10)-O(5)	2.2(2)
		H(5)-H(5)	1.9(3)
H(7)-H(11)	2.1(2)	O(5)-O(10)	2.750(4)
H(7)-H(7)	2.1(1)	O(5)-O(5)	3.006(4)
O(7)-O(11)	2.993(4)		
O(7)-O(7)	2.793(4)	M(1)-O(5)-H(5)	114(7)
		Si(2)-O(10)-H(10)	125(11)
M(1)-O(7)-H(7)	125(1)		
M(2)-O(11)-H(11)	118(4)		

Hydrogen atom positions

The positions of hydrogen atoms are depicted in Figure 3. All donor oxygen-hydrogen bonds in pumpellyite are located in mirror planes parallel to (010). Interatomic distances and angles for hydrogen atoms based on the refined coordinates are presented in Table 8. The distances O(donor)-H are only 0.7(1)Å or 0.6(2)Å. While the hydrogen atoms are located in the general vicinity of these positions, it appears that these refined positions are not as accurate as their precision might imply.

The oxygen atoms connected with these hydrogens are consistent with the results deduced from bond-valence calculations (Allman and Donnay, 1971 and Baur, 1971). Table 9 shows the valence sums recalculated by Donnay and Allman's method (1970). The sums for O(5) and O(7) are close enough to the expected value of 1.0 for a hydroxyl group, while those for O(11) and O(10) are 1.3 v.u.. Substi-

Table 9. Estimated bond valence *** (v.u.) in pumpellyite. The numbers in the left superscripts give the number of identical bonds reaching the anion; the numbers in the right superscripts give the number of identical bonds emanating from the cation

cations anions	Ca (1)	Ca (2)	M (1)	M (2)* (M(2)**)	Si (1)	Si (2)	Si (3)	Ev c	anion chemistry
O (1)		^{x2} 0.36	0.56		^{x2} 1.06			1.98	O ²⁻
O (2)	^{x2} 0.28	^{x2} 0.31		^{x2} 0.40 (0.40)		^{x2} 1.01		2.00 (2.00)	O ²⁻
O (3)	^{x2} 0.30		0.54				^{x2} 1.03	1.87	O ²⁻
O (4)	0.29		^{x2} 0.35		0.95			1.94	O ²⁻
O (5)			^{x2} 0.54					1.08	OH ⁻
O (6)		0.14	^{x2} 0.47				0.97	2.05	O ²⁻
O (7)			^{x2} 0.55					1.10	OH ⁻
O (8)	0.24				0.93	0.94		2.11	O ²⁻
O (9)		0.25		^{x2} ^{x2} 0.42 (0.41)			0.98	2.07 (2.05)	O ²⁻
O (10)		0.29				1.03		1.32	OH ⁻ #
O (11)	0.31			^{x2} ^{x2} 0.53 (0.49)				1.37 (1.29)	OH ⁻ #
Ev a	2.00	2.02	3.01	2.70 (2.60)	4.00	3.99	4.01		

*** See Donnay & Allman 1970

** (Al_{0.47}Fe_{0.23}Mg_{0.33})* (Al_{0.43}Fe_{0.22}Mg_{0.33})

See text

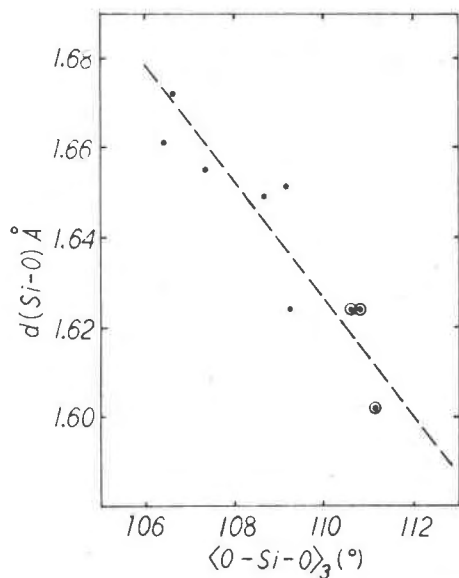


Fig. 5. Pumpellyite, scatter diagram of the observed Si-O bond lengths ($d(Si-O)$) plotted against the average of the three O-Si-O angles common to each bond ($\langle O-Si-O \rangle_3$) after Wan et al. (1977).

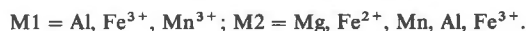
tution, $M_{M(2)}^{2+} + H_{H(11)}^+ + O_{O(11)}^{2-} \rightleftharpoons M_{M(2)}^{3+} + O_{O(11)}^{2-}$, which reduces the number of hydrogen atoms possibly occurs at the M(2) site. Thus the O(11) atom bonded to two M(2) should calculate more than 1.0 v.u.. The sum for O(10) should be explained by the hydrogen bond (O(10)-H(10)---O(5)) which is deduced from the reasonable O(10)-O(5) distance and from the position of the H(10) atom. Therefore the O(5) atom is the acceptor atom for the H(10) atom, and is simultaneously the donor atom for the H(5) atom. A donor and acceptor atom such as O(5), can be seen in afwillite (Malik and Jeffery, 1976) and rosenhahnite (Wan et al., 1977). The acceptor atoms for the other hydrogen atoms can be inferred (two O(3) atoms for H(7) and two O(1) atoms for H(5)), though the proton's positions is not accurately determined.

The double tetrahedral unit, $Si_2O_6(OH)$, has a hydroxide group directly attached to the silicate tetrahedron in our crystal and perhaps in other pumpellyites. The silicate tetrahedron with a hydroxide group has been found in several minerals. For instance, single tetrahedra ($SiO_3(OH)$) occur in afwillite, double tetrahedra ($Si_2O_6(OH)$) in killaite (Taylor, 1977), triple tetrahedra ($Si_3O_8(OH)_2$) in rosenhahnite, and single chains ($Si_3O_8(OH)$) in pectolite (Takéuchi and Kudoh, 1977). Wan et al. (1977) showed that Si-OH(non-br) bonds were significantly longer than the Si-O(non-br) bonds in rosenhahnite. This tendency, however, is not evident in pumpellyite, although we must pay attention to the temperature factor for O(10). Figure 5 (the same as that for rosenhahnite) shows that the shorter bond involves the wider O-Si-O angles. Consequently the Si(2)-O(10) distance is not specifically anomalous.

Chemical formula of pumpellyite

Based on the present crystal structure analysis the chemical formula of Al-rich pumpellyite should be written as $(Ca, Mn)CaAl_2(OH)_2(Mg, Fe^{2+}, Al, Fe^{3+})[(OH), O]SiO_4Si_2O_6(OH)$ with four formula units per unit cell.

We also suggest the following general formula for the collective pumpellyite group, which include special Mn-rich pumpellyites reported by Togari and Akasaka (1982):



Pumpellyite has the following characteristics: both isolated $[SiO_4]$ and double $[Si_2O_6(OH)]$ tetrahedra; one of two kinds of octahedral sites is occupied by aluminum ion in preference to any other; the other site is occupied by both divalent and trivalent ions such as Mg^{2+} , Fe^{2+} , Mn^{2+} , Mn^{3+} , Fe^{3+} , and Al^{3+} ; and the electric charge of the latter site is compensated by the amount of hydrogen atoms.

Acknowledgments

We are grateful to Dr. K. Sakurai for offering the samples investigated, to Prof. P. B. Moore and Dr. R. M. Hazen for critical reading of this manuscript, and to Prof. S. Banno and Drs. K. Kihara, H. Horiuchi and K. Koto for their encouragement. Discussion with and information presented by Profs. G. Donnay, J. D. H. Donnay, and F. Kanamaru and Mr. K. Aiba are much appreciated. The computations were performed at the Computer Center of the Kanazawa University and at the Crystallographic Research Center, Institute of Protein Research, Osaka University. This work was supported in part by a Grant-in-Aid for Scientific Research from the Ministry of Education in Japan.

References

- Aiba, K. (1982) Sanbagawa metamorphism of the Nakatsu-Nanokawa District, the Northern Subbelt of the Chichibu Belt in Western Central Shikoku. *Journal of the Geological Society of Japan*, 88, 875-885.
- Allman, R. and Donnay, G. (1971) Structural relations between pumpellyite and ardennite. *Acta Crystallographica*, B27, 1871-1875.
- Baur, W. H. (1971) Prediction of bond length variations in silicon-oxygen bonds. *American Mineralogist*, 56, 1573-1599.
- Coombs, D. S. (1953) The pumpellyite mineral series. *Mineralogical Magazine*, 30, 113-135.
- Coombs, D. S., Nakamura, Y. and Vuagmat, M. (1976) Pumpellyite-actinolite facies shists of the Taveyanne Formation near Loèche, Valais, Switzerland. *Journal of Petrology*, 17, 440-471.
- Coppens, P. and Hamilton, W. C. (1970) Anisotropic extinction correction in the Zachariasen approximation. *Acta Crystallographica*, A26, 71-83.
- Deer, W. A., Howie, R. A. and Zussman, J. (1962) *Rock-forming Minerals*, Vol. 1, Ortho- and Ring Silicate. Longmans, London.
- Dollase, W. A. (1968) Refinement and comparison of the structures of zoisite and clinozoisite. *American Mineralogist*, 53, 1882-1898.
- Donnay, G. and Allman, R. (1970) How to recognize O^{2-} , OH^- , and H_2O in crystal structures determined by X-Rays. *American Mineralogist*, 55, 1003-1015.

- Galli, E. and Alberti, A. (1969) On the crystal structure of pumpellyite. *Acta Crystallographica*, B25, 2276–2281.
- Gottardi, G. (1965) Die Kristallstruktur von Pumpellyit. *Tschermaks Mineralogische und Petrographische Mitteilungen*, 10, 115–119.
- Howells, E. R., Phillips, D. C. and Rogers, D. (1950) The probability distribution of X-ray intensities, II. Experimental investigation and the X-ray detection of centers of symmetry. *Acta Crystallographica*, 3, 210–214.
- Ishizuka, H. (1981) Greenstones from the Idonnappu Formation along the River Oku-Niikappu in the axial zone of Hokkaido, Japan. Reprinted from the *Memoirs of the Faculty of Science, Kochi University, Series E, Geology*, 2, 1–22.
- Kawachi, Y. (1975) Pumpellyite–actinolite and contiguous facies metamorphism in part of Upper Wakatipu District, South Island, New Zealand. *New Zealand Journal of Geology and Geophysics*, 18, 401–441.
- Kuniyoshi, S. and Liou, J. G. (1976) Burial metamorphism of the Karmutsen Volcanic Rocks, northeastern Vancouver Island, British Columbia. *American Journal of Science*, 276, 1096–1119.
- Liou, J. G. (1979) Zeolite facies metamorphism of basaltic rocks from the East Taiwan Ophiolite. *American Mineralogist*, 64, 1–14.
- Liou, J. G., Lan, C. Y., Suppe, J. and Ernst, W. G. (1977) The East Taiwan Ophiolite; its occurrence, petrology, metamorphism and tectonic setting. *Mining Research Service Organization Special Report*, No. 1, 221.
- Malik, K. M. A. and Jeffery, J. W. (1976) A re-investigation of the structure of awillite. *Acta Crystallographica*, B32, 475–480.
- Moore, P. B. (1971) Julgoldite, the Fe^{2+} – Fe^{3+} dominant pumpellyite. *Lithos*, 4, 93–99.
- Nakajima, T. (1982) Phase relations of pumpellyite–actinolite facies metabasites in the Sanbagawa Metamorphic Belt in Central Shikoku, Japan. *Lithos*, 15, 267–280.
- Passaglia, E. and Gottardi, G. (1973) Crystal chemistry and nomenclature of pumpellyites and julgoldites. *Canadian Mineralogist*, 12, 219–223.
- Shannon, R. D. (1976) Revised effective ionic radii and systematic studies of interatomic distances in halides and chalcogenides. *Acta Crystallographica*, A32, 751–767.
- Takéuchi, Y. and Kudho, Y. (1977) Hydrogen bonding and cation ordering in Magnet Cove pectolite. *Zeitschrift für Kristallographie*, 146, 281–292.
- Taylor, H. F. W. (1977) The crystal structure of killalaite. *Mineralogical Magazine*, 41, 363–369.
- Togari, K. and Akasaka, M. (1982) On the mangano-pumpellyite (in Japanese). *Mineralogical Society of Japan 1982 Annual Meeting Abstracts*, 139.
- Wan, C., Ghose, S. and Gibbs, G. V. (1977) Rosenhahnite, $\text{Ca}_3\text{Si}_3\text{O}_8(\text{OH})_2$: crystal structure and the stereochemical configuration of the hydroxylated trisilicate group, $[\text{Si}_3\text{O}_8(\text{OH})_2]$. *American Mineralogist*, 62, 503–512.
- Zen, E-an (1974) Prehnite- and pumpellyite-bearing mineral assemblages, west side of Appalachian metamorphic belt, Pennsylvania to Newfoundland. *Journal of Petrology*, 15, 197–242.

*Manuscript received, September 18, 1984;
accepted for publication, April 25, 1985.*